DEUTSCHES ELEKTRONEN-SYNCHROTRON DESY

DESY SR-79/12
July 1979

A Scanning Ultrasoft X-Ray Microscope with Large Aperture Reflection Optics for Use with Synchrotron Radiation

by

R.-P. Haelbich, W. Staehr, C. Kunz

Deutsches Elektronen-Synchotron DESY, Hamburg
and
II. Institut für Experimentalphysik der Universität Hamburg

NOTKESTRASSE 85 · 2 HAMBURG 52

To be sure that your preprints are promptly included in the
HIGH ENERGY PHYSICS INDEX ,
send them to the following address (if possible by air mail) :

DESY
Bibliothek
Notkestrasse 85
2 Hamburg 52
Germany

A Scanning Ultrasoft X-Ray Microscope with Large Aperture Reflection Optics for Use with Synchrotron Radiation [+]

R.-P. Haelbich, W. Staehr and C. Kunz

Deutsches Elektronen-Synchrotron DESY, 2000 Hamburg 52, West Germany
and II. Institut für Experimentalphysik der Universität Hamburg

Newly developed multilayer interference coatings allow to use the advantages of normal incidence optics also in the ultrasoft x-ray region: small aberrations and large aperture. For example, a Schwarzschild type objective with two spherical reflectors allows under certain geometrical conditions to produce an aberration free, highly demagnified image of a light source. This can be used as a probe for scanning a sample while the transmitted light is recorded to form the image. Since the objective has an efficiency much smaller than one, scanning is preferred to direct imaging to reduce radiation damage in biological specimens. Synchrotron radiation, especially from a storage ring like DORIS, is a bright tunable source which can yield an image below 1000 Å in diameter with about 10^7 photons/second in a 5% band around λ = 100 Å. Demagnification should be achievable in two steps: (1) High efficiency grazing incidence mirror and (2) Multilayer coated Schwarzschild objective. A prototype has been optically tested and is presently installed at the synchrotron DESY.

+ will be published in the Annals of the New York Academy of Sciences.

Presented at the Conference on Ultrasoft X-ray Microscopy, New York Academy of Sciences, June 13-15, 1979.

1. Introduction

Imaging with soft x-rays for microscopical purposes is in principle possible by shadow casting (1, 2), Fresnel zone plates (3), a pinhole in combination with a scanning drive (4), holography (5) and grazing incidence mirrors (6, 7, 8). Since the reflectivities of mirror coating materials in the wavelength range below 100 Å are smaller than a tenth of a percent for normal-incidence, such mirrors have not been considered so far. By use of multilayer interference coatings (9, 10) with enhanced, wavelength selective reflectivity, it seems possible to extend the application of such mirrors down to λ = 50 Å and to profit thereby from the advantages of normal incidence mirrors: smaller aberrations and larger apertures. A Schwarzschild type objective, for example, with two spherical concentric mirrors under certain geometrical conditions is almost free from aberrations and can be produced with good accuracy because of the spherical shape of the mirrors. Since, however, two reflections are necessary, the efficiency of such an objective will be small in any case. If used for direct imaging, the specimen would be irradiated by a number of photons two or three orders of magnitude higher than that contributing to the formation of the image. Therefore, we prefer a scanning version of such a microscope and use the objective to form a highly demagnified image of the source. In the next section, the experimental setup is outlined, in Sections 3 and 4 details about multilayer interference coatings and the Schwarzschild type objective are given and in Section 5 the prototype of a microscope, which is presently under construction at the DESY synchrotron, is described.

2. Principle of the Setup of a Microscope at a Synchrotron Radiation Source

Figure 1 shows the envisaged setup of the microscope at the storage ring DORIS. The electron beam at the tangential point has a cross-section of 1 x 3 mm^2 which defines the source dimensions. The incident light first is reflected by a plane mirror. With the angle of incidence properly adjusted the unused high energy part of the spectrum which might damage the following expensive elliptical or parabolic mirror is eliminated. This second mirror forms a roughly hundred times reduced image of the source. Since the mirror is used at grazing incidence, the size of the image is limited by imaging errors The blurr of the image is cut off by a pinhole with a few micrometers in diameter. In addition, this aperture allows vaccum separation of the ultrahigh vacuum beamline from the experimental chamber which is kept at normal vacuum conditions. The second demagnification is achieved by the Schwarzschild type objective. Under optimal conditions, the size of the image is diffraction limited. At λ = 100 Å with a numerical aperture (N.A.) of .3 the diffraction disc has a radius of 200 Å (the radius of the first dark ring). The aberrations are negligible and the modifications introduced by the central obstruction of the beam will be discussed in Section 4.

Since the thus formed light spot cannot be easily moved across the sample, a scanning motion of the whole sample must be applied. The scanning mechanism can be driven by precision screws, piezoelectrically or electromagnetically. The most important feature is not linearity but reproducibility, so that one line scan fits the adjacent one. The transmitted light or the emitted photoelectrons can be recorded with

a detector which controls the brightness of a cathode ray tube while the beam deflection is coupled to the scan generator.

A source of 1 mm size has to be demagnified by a factor of 2.5 x 10^4 to form an image of 400 Å in diameter. Since the product of spot size and aperture are not affected by imaging, this implies that the microscope can accept only an angle of .2 mrad of the incident radiation which is less than one fifth of the natural vertical divergence of the synchrotron radiation from a storage ring like DORIS at λ= 100 Å. It appears possible to reduce the vertical height of the DORIS electron beam further by a factor of 3 which will reduce the necessary demagnification and thereby increase the acceptable angle by the same factor. In the future, storage ring beam sizes below 100 µm will become available. This small acceptance angle of a scanning microscope is the reason why the brightness of the source rather than the overall intensity is the relevant parameter. Synchrotron radiation sources are ideal in this respect.

With DORIS as a source we obtain a brightness of 10^{21} photons/sec x cm^2 x sterad x eV at λ = 100 Å. A microscope with .3 N.A. and a light spot of 400 Å in diameter which works with roughly monochromatized light of 5% bandwidth can accept about 4 x 10^{11} photons/sec. If we further assume that the grazing incidence reflections reduce the intensity by a factor 0.5 each and the objective has an efficiency of 0.1%, we obtain 10^7 photons/sec. focussed in the scanning spot on the sample. This would allow a scanning speed of more than 1000 points/sec. with reasonable statistics.

In addition to the reduction of radiation damage as mentioned above, scanning was chosen because of the following advantages:

(1) The detector has not to be position sensitive, but may be optimized for maximum efficiency.

(2) The information is at once available and makes real time microscopy easy.

(3) With on-axis imaging only spherical aberrations come into play.

(4) Signal processing is easy to accomplish.

(5) Interesting parts of the image can selectively be scanned with higher speed or better quality of the image if the operator wants to do so.

3. Multilayer Interference Coatings

In x-ray physics crystals are good reflectors when all lattice planes add in phase to the reflected wave. In order to be more flexible in the choice of lattice constants, it is possible to evaporate alternating layers of highly (in our case ReW) and weakly (in our case C) absorbing materials (12). As with natural crystals, the superposition of the incident and the reflected beam produces a standing wavefield with the highly absorbing layers in the nodes, thus the penetration depth is considerably enlarged and a great number of layers contributes to the reflected beam.

Fig. 2 shows the near-normal-incidence reflectivity of a multilayer interference coating with 3, 5 and 7 layers of ReW and of C in comparison to a single thick film of ReW (11). The peak reflectivity is increasing with the number of periods, but the width of the peaks is decreasing and therefore the integral under the reflectivity curve is growing more slowly than the peak reflectivity. Thus, the reflector additionally acts as a coarse monochromator, its bandwidth depending on the number of periods. In order to get good contrast in soft x-ray microscopy, this coarse monochromacy is necessary and the multilayer coatings on the objective mirrors make extra monochromatization unnecessary. A filter (for example Carbon) is needed to suppress long wavelength radiation. In order to change the wavelength , however, one has to take another objective optimized for a different wavelength.

Examination of scattered light from these coatings has shown that the surface roughness induced by these films is so small that normal incidence reflection down to $\lambda = 50$ Å appears to be feasible (11). For the fabrication of multilayer films optimized for such short wavelengths a good method of thickness control during evaporation is of utmost importance (see Ref. 13).

4. The Schwarzschild Type Objective

Schwarzschild type objectives (14) have been used for 40 years in microscopy, especially for infrared or ultraviolet light (15). Fig. 3 shows an objective with two concentric spherical mirrors. The smaller convex mirror forms a strongly demagnified virtual intermediate image,

the larger concave mirror forms a weakly enlarged real image of this virtual image. The aberrations of the concave and convex mirror have opposite signs and compensate each other. In a concentric mounting where the radii of the convex r_1 and the concave r_2 mirror obey the following relation with the distance s of the object to the convex mirror surface

$$\frac{r_1}{r_2} = -1.5 + \frac{r_1}{r_1 - s} + \sqrt{1.25 - \frac{r_1}{r_1 - s}}$$

the objective is free from third order spherical aberrations, coma and astigmatism (16). This geometrical condition implies, however, that about 21% of the central area of the objective is obstructed. This influences the intensity distribution in the diffraction pattern of the objective. In Fig. 4 the change of intensity distribution from an unobstructed circular aperture to an annular aperture with 21% areal obstruction is shown (14). For the latter, the diamter of the Airy disk is even smaller, but part of the intensity from the central maximum is shifted to the rings. For objects with sufficient contrast point resolution is therefore improved. This has been demonstrated in an optical scanning microscope by Brakenhoff et al. (17).

The most critical points in fabrication of such an objective are optical figure and surface roughness. When reflection occurs at a mirror element which is displaced by an amount δ from the ideal surface, the optical path length is changed by $2\delta \sin\theta$ where θ is the grazing angle of incidence. Since we use the objective at normal incidence, the quality of the image is strongly depending on these deviations δ . This retardation error should be less than $\lambda/4$ in order to have a diffraction limited image. Then δ should be smaller than $\lambda/8\sqrt{2}$ for each mirror. For visible radiation

normally taken for testing the optical figure, this means at least $\lambda/600$. This is an extreme requirement and the only chance to obtain components with this accuracy will be with spherical mirrors whose shape is self generating. This is the main reason why we prefer an objective with two reflections over a single ellipsoidal mirror.

Surface roughness produces scattered light which reduces reflectivity and contrast. Even an extremely well polished surface with 10 Å rms surface roughness will produce more than 80% scattered light at $\lambda = 100$ Å at normal incidence (18). Plane and spherical surfaces are generally produced with the largest possible smoothness.

An additional advantage of the Schwarzschild type objective is its great working distance, since its principal planes coincide in the common center of the mirrors which lies outside the objective on the side where the specimen is placed. Typical parameters of a Schwarzschild type objective are given in Table 1.

5. The Prototype

In order to learn more about the technical problems involved, the prototype of such a microscope has been constructed. In a first step this instrument was tested with visible light. The pinhole between the grazing incidence mirror and the objective is illuminated with a He - Ne Laser. The objective is a commercial one (Ealing) designed for applications in the infrared and ultraviolet. It has a numerical aperture of .28 and the radii of curvature of the mirrors are 17 mm and 45 mm. The fulfilment of the condition for disappearing aberrations, as mentioned above, is unimportant for this objective since the resolution in the visible is already restricted by diffraction and in

the soft x-ray region by the poor optical figure of the mirrors.

Scanning of the sample is achieved in two ways. First, there is a mechanical stage driven by micrometer screws with a DC motor and the position is measured by carbon film potentiometers or inductive displacement transducers. The potentiometers have a resolution of about .5 μm, the inductive transducers have a resolution better than 1000 Å. Alternatively, the sample can be directly attached to two piezoelectric transducers which consist of stacks of piezoelectric disks. They have a maximum range of displacement of 40 μm and their resettability is better than 1000 Å. But they show an unusual time characteristic with a very long time constant for the last part of their motion, this lies in the order of minutes. Therefore, control of the displacement without transducers only by the applied voltage is difficult.

Compared to normal objectives for optical microscopy the Schwarzschild type objective used has a very low numerical aperture and therefore the first dark ring has a radius of 1.2 μm at λ = 632.8 nm when the central obstruction is considered. This value is usually taken as resolution limit.

Fig. 5 demonstrates the edge resolution of the microscope. For this line scan of a razor blade edge the scanning stage was driven by precision screws and the position monitored by inductive transducers. The flatter parts of the curve surrounding the central steep part correspond to the first dark diffraction ring of the objective and show that the radius is 1.2 μm as expected.

In order to keep the expense for data handling as small as possible, we abstained from displaying the transmission signal on a TV screen. The image is recorded through line scans on an x-y recorder. By scanning many lines equivalently shifted on the sample and on the x-y recorder a so-called y-modulation image is obtained. Such an image of a support grid of a transmission grating with about 30 μm periodicity is shown in Fig. 6 and demonstrates the usefulness of this procedure. The transmission grating itself has 1 μm periodicity, therefore its structure is not resolved.

At the synchrotron we use a grazing incidence monochromator (19) in zero order which focusses the beam with a paraboloid onto the pinhole which is exchanged for the exit slit of the monochromator. A second Schwarzschild type objective with better optical figure than that used for the optical tests is available. It will be coated with a multilayer coating optimized for λ = 170 Å.

6. Summary

A project for building an ultrasoft x-ray microscope was introduced. The outstanding features are (1) normal incidence objective coated with multilayer films, (2) relatively high aperture, and (3) scanning principle. The present studies with a prototype serve to evaluate the technical and physical feasibility and should allow comparison with other approaches towards soft x-ray microscopy.

We thank E. Spiller for several discussions and exchange of ideas.

References

1 Feder, R., E. Spiller, J. Topalian, A.N. Broers, W. Gudat, B.J. Panessa, Z.A. Zadunaisky &. J. Sedat. 1977. Science 197: 259.

2 Spiller, E. & R. Feder. 1977. In Topics in Appl. Phys. H.J. Queisser, Ed.Vol. 22: 35. Springer Verlag. Berlin, Heidelberg, New York.

3 Schmahl, G., D. Rudolph & B. Niemann. 1978. J. Physique Colloq. 39: C4-202

4 Horowitz, P. & J.A. Howell. 1972. Science 178: 608

5 Aoki, S. & S. Kikuta. 1974. Japan. J. Appl. Phys. 13: 1385.

6 Kirkpatrik, P. & A.V. Baez. 1948. J. Opt. Soc. Am. 38: 766

7 Wolter, H. 1952. Ann. Phys. 10: 94

8 Boyle, M.J. & H.G. Ahlstrom. 1978. Rev. Sci. Instrum. 49: 746

9 Haelbich, R.P. & C. Kunz. 1974. Opt. Commun. 17: 287

10 Spiller, E. 1976. Appl. Opt. 15: 2333

11 Haelbich, R.-P., A. Segmüller & E. Spiller. 1979. Appl. Phys. Lett. 34: 184.

12 Spiller, E. 1972. Appl. Phys. Lett. 20: 365

13 Spiller, E. & R.-P. Haelbich. 1979. This conference

14 Riesenberg, H. 1957. In Jenaer Jahrbuch 1956. VEB Carl Zeiss Jena, Ed.: 30. VEB Gustav Fischer Verlag, Jena.

15 Norris, K-P. 1955. Research 8: 94.

16 Grey, D.S. 1950. J. Opt. Soc. Am. 40: 283

17 Brakenhoff, G.J., P. Blom & C. Bakker. 1978. In Proceedings of ICO-11 Conference: 215. Madrid, Spain.

18 Bennett, H.E. & I.O. Porteus, 1961. J. Opt. Soc. Am. 51: 123

19 Dietrich, H. & C. Kunz. 1972. Rev. Sci. Instrum. 43: 434

TABLE 1

Example of typical parameters of a Schwarzschild type objective with two spherical concentric mirrors.

Radius of curvature of convex mirror	58.2	mm
Radius of curvature of concave mirror	152.5	mm
Object - image distance	1	m
Imaging scale	50	
Numerical aperture	.5	
Diameter of convex mirror	22	mm
Diameter of concave mirror	102	mm

Figure Captions

Fig. 1: Principle of scanning ultrasoft x-ray microscope. Light from a synchrotron radiation source SR is reflected by premirror PM and grazing incidence focussing mirror FM onto the pinhole P. The Schwarzschild type objective SO forms a reduced image of the pinhole on the sample. This is fixed on sample holder SH which is attached to an x-y scanning stage controlled by scan-generator SG. The transmitted light is recorded by detector D, this signal controls the brightness of the cathode-ray tube CRT by amplifier A.

Fig. 2: Measured reflectivity of a single 400-Å-thick ReW film and of a three-, five- and seven layer coating of ReW and C for an angle of incidence $\alpha = 15^{\circ}$. The three and five layer coatings were obtained by shadowing part of the wafer by a shutter during the evaporation. After Ref. 11.

Fig. 3: Diagram of a Schwarzschild type objective with two spherical mirrors which have a common center C. The convex mirror forms a strongly demagnified virtual intermediate image I of the object O. The concave mirror forms a weakly enlarged image I' of I. F: image side focal point.

Fig. 4: Intensity distribution of the diffraction pattern of a non-obstructed circular aperture and an aperture with 21% area obstruction in the center. The central maximum is smaller in diameter in case of central obstruction but part of the intensity is shifted to the rings. The intensity is normalized to 1 at the center of both curves respectively. The coordinate x in the focal plane is measured in wavelength per unit numerical aperture.

Fig. 5: Line scan of a razor blade edge. The scanning table has been moved by precision screws and its position monitored by inductive transducers. The flatter parts of the curve surrounding the central steep part correspond to the first dark diffraction ring of the objective, its radius being 1.2 µm as expected.

Fig. 6: Y-modulation image of a support grid of a transmission grating with about 30 µm periodicity. The transmission grating itself has 1 µm periodicity; therefore its structure is not resolved.

Fig. 1

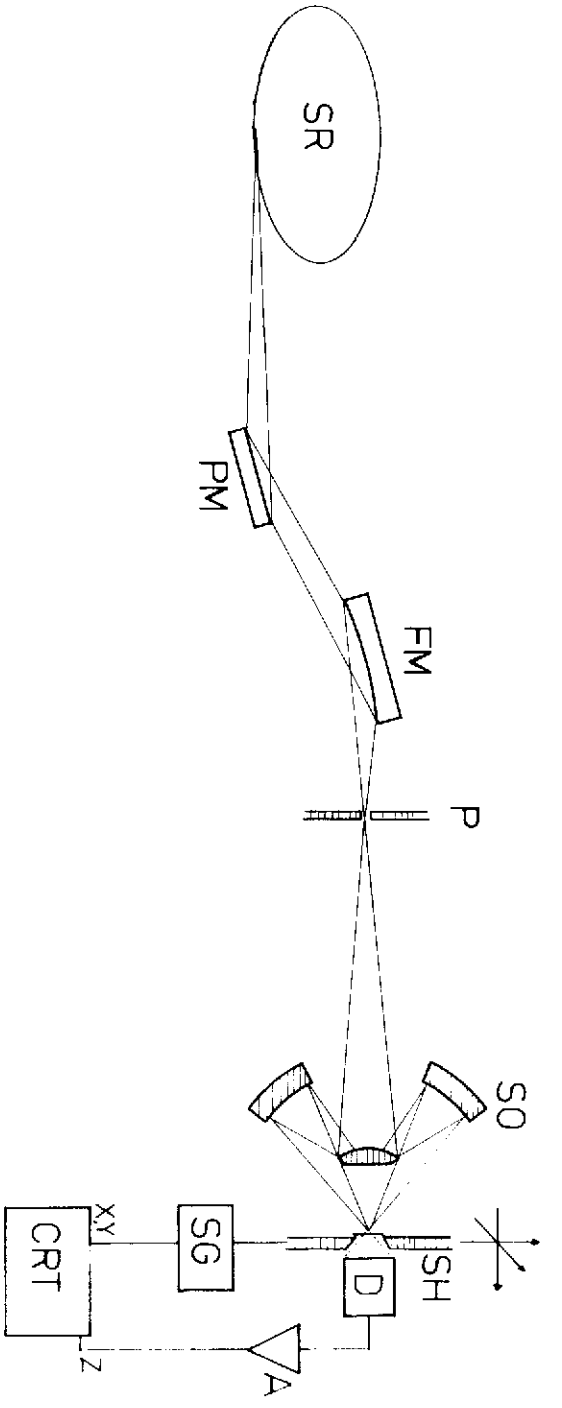

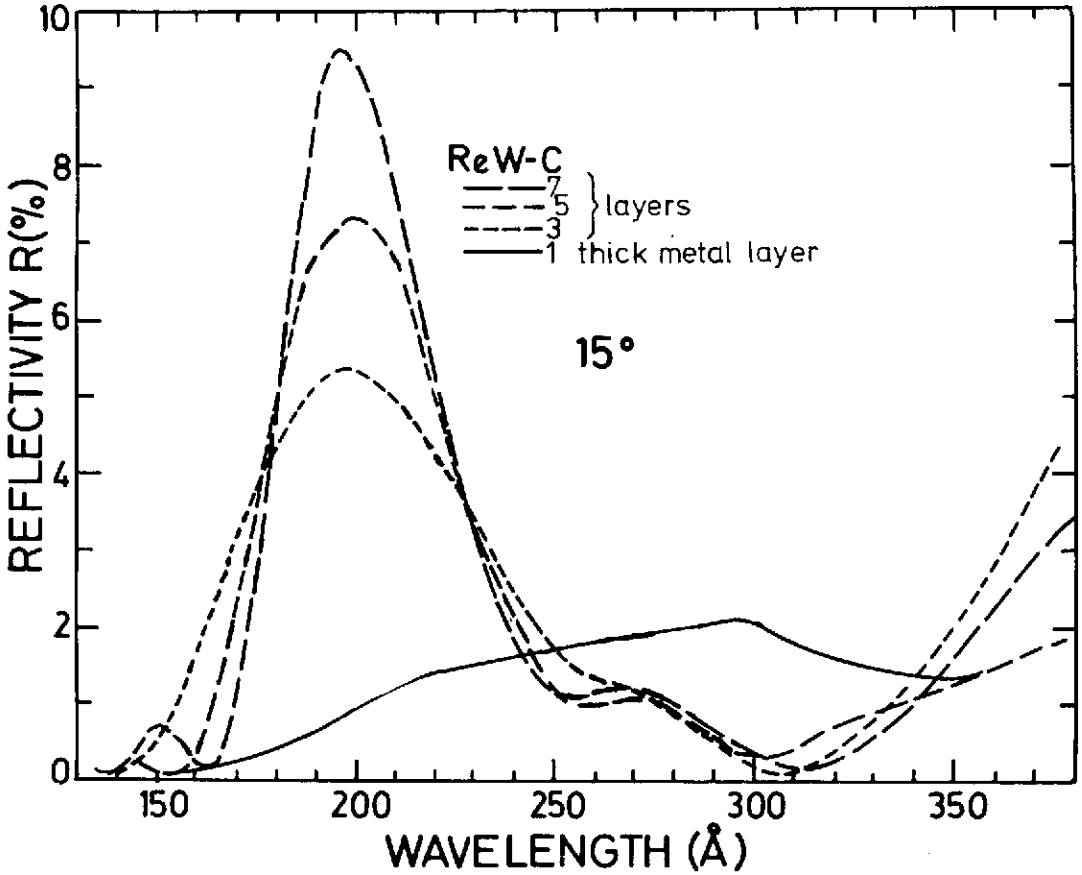
ReW-C
7
5
3
layers
1 thick metal layer
15°
REFLECTIVITY R(%)
WAVELENGTH (Å)
0
2
4
6
8
10
150
200
250
300
350

Fig. 2

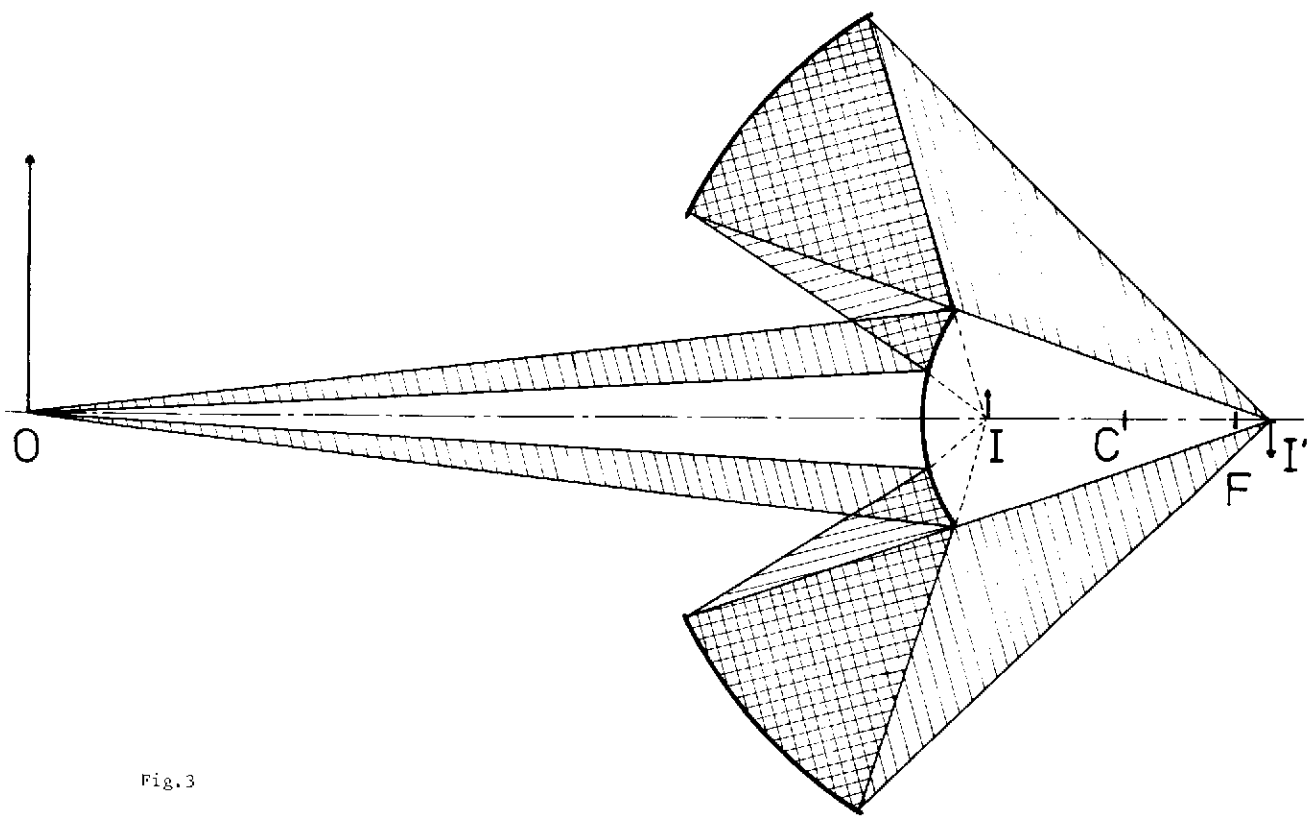
O
I
C
F
I'

Fig.3

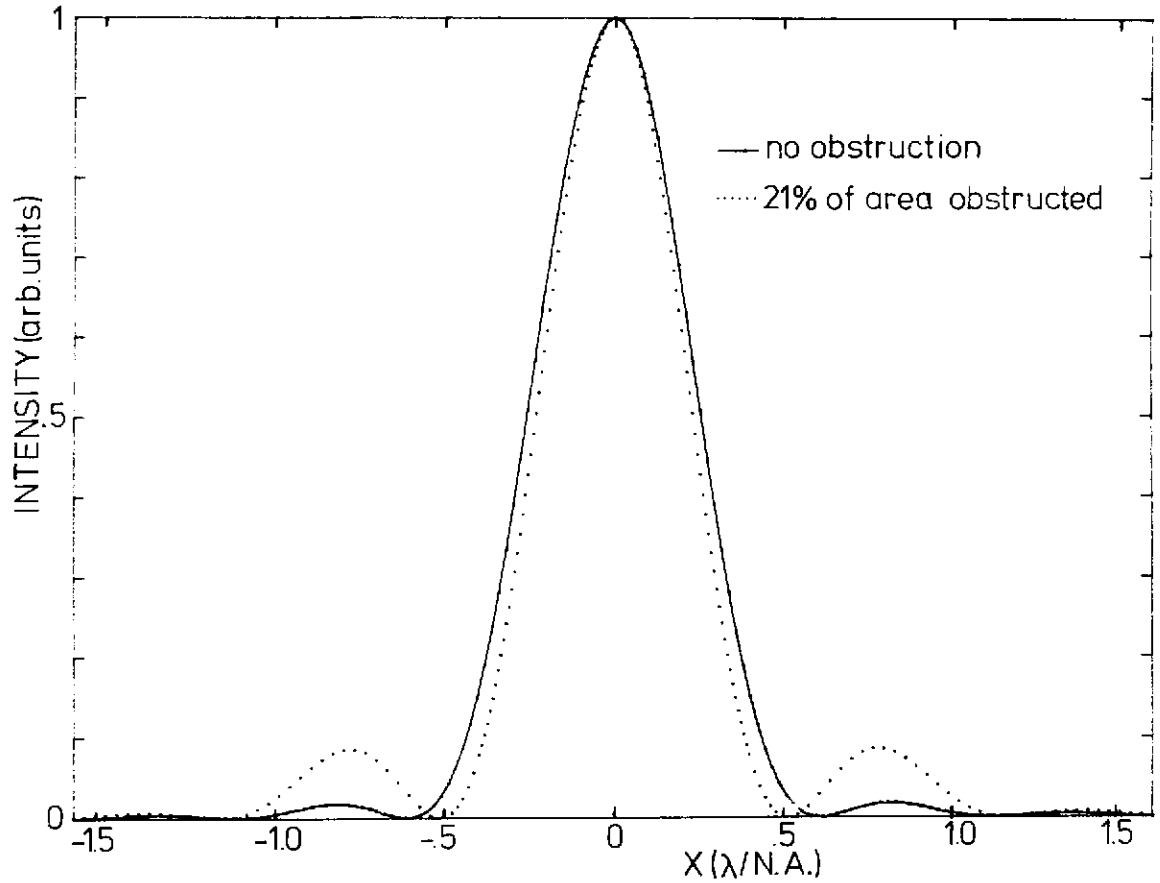
1
.5
0
INTENSITY (arb. units)
no obstruction
21% of area obstructed
-1.5
-1.0
-.5
0
.5
1.0
1.5
X (λ/N.A.)

Fig. 4

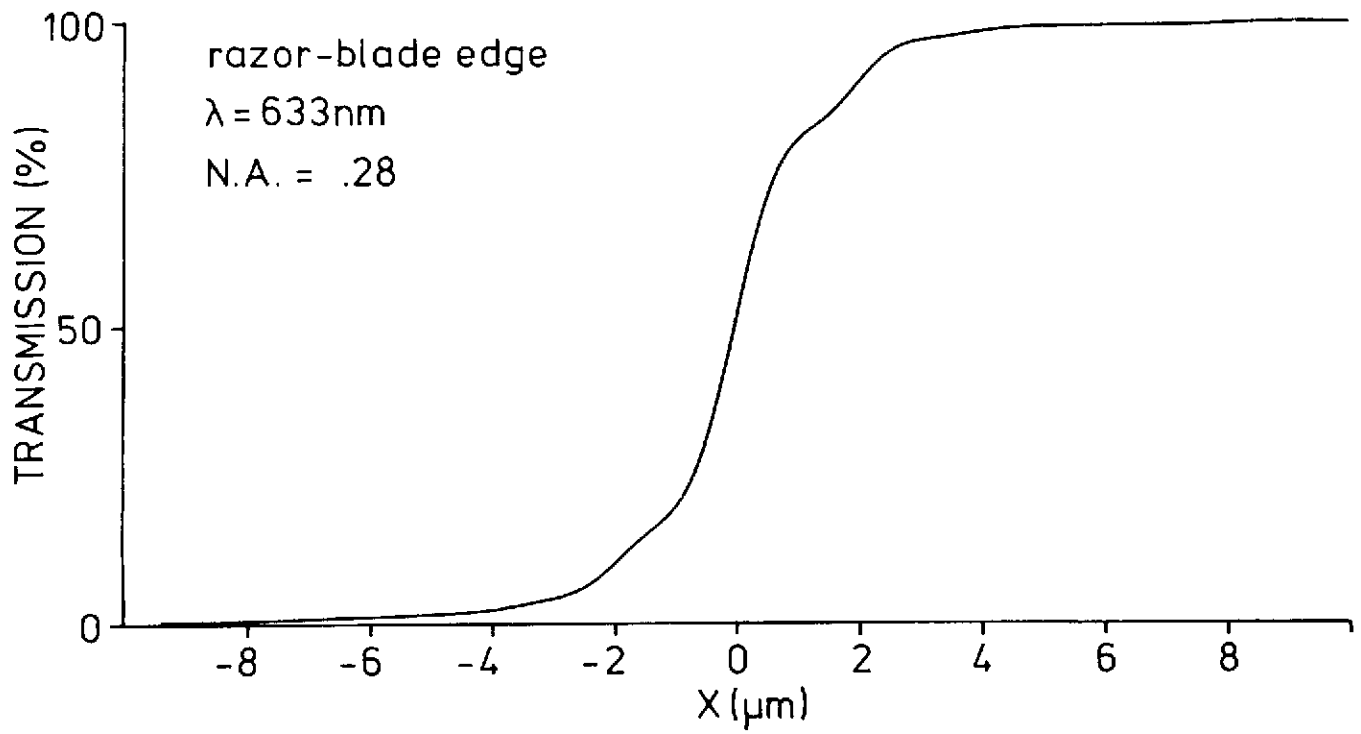
100
50
0
TRANSMISSION (%)
razor-blade edge
λ = 633nm
N.A. = .28
-8
-6
-4
-2
0
2
4
6
8
X (μm)

Fig. 5

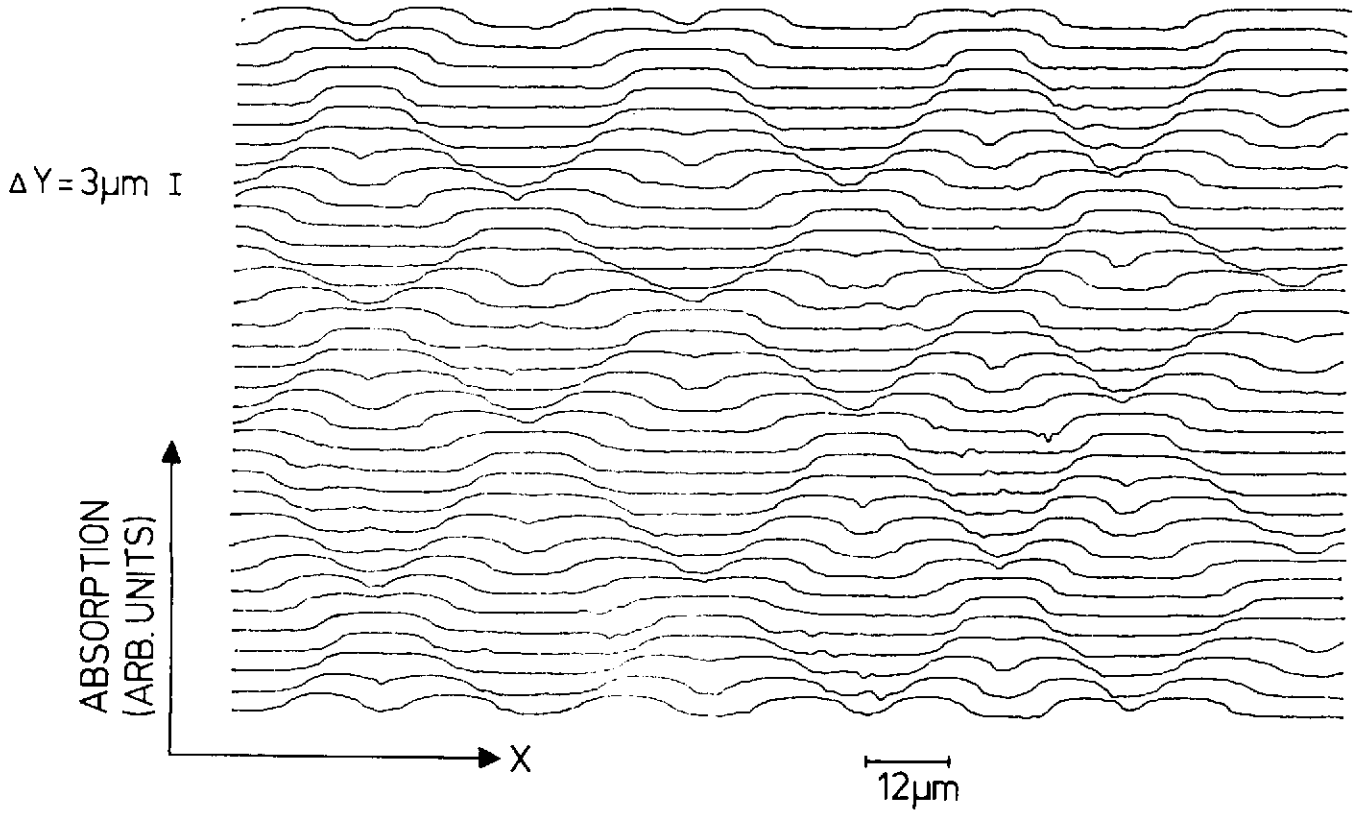

Fig. 6